Journal of Pharmaceutical and Scientific Innovation

www.jpsionline.com (ISSN : 2277 -4572)

Research Article

PHOSPHATE TYPE KIDNEY STONE (BRUSHITE) FORMATION IN GEL: A MORPHOLOGICAL STUDY ON GROWTH PATTERNS

Salman Ahmed [1], Muhammad Mohtasheemul Hasan [1]* and Zafar Alam Mahmood [2]
[1]Department of Pharmacognosy, Faculty of Pharmacy, University of Karachi, Karachi, Pakistan
[2]Colorcon Limited – UK, Flagship House, Victory Way, Crossways, Dartford, Kent, DA26 QD- England
*Corresponding Author Email: mohassan@uok.edu.pk

DOI: 10.7897/2277-4572.06355

Received on: 27/05/16 Revised on: 06/06/16 Accepted on: 11/06/17

ABSTRACT

Brushites are most commonly found phosphate stones in the kidneys, ureters and urinary bladder. The study was conducted to observe the possible growth patterns of brushite crystals in gel for 14 days. The crystals formation was observed as a bullet, needle, platy, columnar shaped and their aggregates. These shapes were further explained by Magono and Lee meteorological classification. Beside the morphology, average size, number and weight of crystals were also observed at 7th and 14th day. Energy Dispersive X-ray, Fourier Transform Infra Red spectroscopy and Scanning Electron Microscopy were used to characterize the crystals. These results can help to determine the promotion, modulation and inhibition of the crystals which will be helpful to evaluate the risk factors and prophylactic management of brushite type urinary stones.

Keywords: Crystal morphology, characterization, calcium hydrogen phosphate dihydrate, urolithiasis.

INTRODUCTION

Gallstones, gout and urinary stone diseases are associated with the presence of crystals contribute to tissue damage followed by successive aggregation, crystal growth, blockage of ducts and pain[1]. Urolithiasis is a common clinical problem with high recurrence. Urinary stones are composed of insoluble crystalline compounds which include inorganic phases such as oxalate, phosphate and urate salts while organic matrix include proteins, lipids, polysaccharides and cellular components such as cystine, xanthine, calcium carbonate or hippuric acid[2,3]. The damaged glycosaminoglycan layer favors the attachment of calcium phosphates, glycoprotein aggregates and cellular debris to the urothelial surface. Successive adhesion and aggregation results comparatively larger particle to form urinary stones[4]. Calcium phosphate urinary stones which are about 15% of urinary stones are found in the form of brushite, dahllite, hydroxyapatite, whitlockite and octacalcium phosphate. Brushite crystals form urinary stone, promote whewellite (calcium oxalate) stone formation and act as a precursor to form apatite and octacalcium phosphate type urinary crystals[5,6]. Among all urinary phosphate crystals, brushite has the greater hardness and difficult to remove surgically by the shock wave and ultrasonic lithotripsy. Brushite crystals grow rapidly with high recurrence rate and cause a significant degree of renal tissue injury as compare to other forms of stone[7,8]. Brushite crystals induce apoptosis of renal proximal tubular epithelial cells and collecting ducts which create sites for crystal attachment followed by growth and maturing into brushite and whewellite stones[6].

Crystal growth in gel is a simple and inexpensive *in vitro* technique which provides direct access to observe the crystallization process resembled to human physiological conditions[9,10]. Gel technique has been successfully applied to grow pathologic crystals. Although, brushite crystals has already been grown in gel[5,11]. Severe renal tissue injury, high recurrence rate and difficulty in surgical removal of brushite stone potentiate us to study their different morphological features as an applied approach to evaluate risk factors and natural prophylactic management in future.

MATERIALS AND METHODS

Chemicals

Calcium chloride dihydrate, orthophosphoric acid and sodium silicate solution (Merck, Germany).

Instruments

Glass test tubes of 25mm diameter and 150mm length; IR Prestige-21 FTI-R Spectrophotometer Shimadzu; JSM-6380A Scanning Electron Microscope and EDS EX-54175 JMU, JEOL Japan; Nikon Eclipse E 400 binocular microscope, Japan.

Crystal growth and characterization

The single diffusion gel method was used with some modifications[5]. Sodium meta silicate solution of 1.06 specific gravity and 1M orthophosphoric acid solution were mixed to prepare gel medium. After gel formation, 20ml of 1M calcium chloride solution was gently poured along with the wall of test tube. The test tube was capped and observed at 7th and 14th day. The carefully recovered crystals were washed, dried and characterized by FT-IR, SEM and EDS.

Statistical analysis

Number, size and weights of crystals are expressed as mean ± standard error of mean and were analyzed by unpaired student t-test.

Table 1: Growth patterns of brushite crystals

Growth periods (days)	Average crystals per vessel			Crystal density	
	Number	Weight (mg)	Size (mm)	On the basis of number	On the basis of length
07	7.40±0.50*	31.76±0.46*	2.91±0.27*	N2c and R2a > N1a and R1a > C1c > N2a and R1c > P7a > C1d.	N2c > R1c > R2a > C1c > R1a > N2a > P7a > N1a > C1d.
14	8.80±0.96*	86.93±0.33*	5.87±0.88*	N1e > C1g > N1c > N2c > P1b > C1h and P7a > N1a.	N1a> C1h > N2c > P1b > C1g > N1e > P7a > N1c.
C1c: solid bullet, C1d: hollow bullet, C1g: solid thick plate, C1h: thick plate of skeletal form, N1a: elementary needle, N1c: elementary sheath, N1e: long solid column, N2a: combination of needles, N2c: combination of long solid column, P1b: sector plate, P7a: radiating assemblage of plates, R1a: rimed needle, R1c: rimed plate or sector, R2a: densely rimed plate or sector. All values represent mean ± SEM of n=5; **P*<0.01 showing significant values using unpaired student's *t*-test.					

Table 2: FT-IR wave numbers and vibrations assignment of brushite crystals

Wave numbers (cm-1)			Bonds / vibrations
Standard	Grown	Reported values[5,15,16]	
3541.31	**3541.31**	3539.80,3543.16,3544	O-H stretching (weakly H bonded OH vibrations) of water
3485.37	3487.30	3487.10,3487.57,3489	
3290.56	3282.84	3282.79,3284	
-------	3161.33	3166.70,3167	
2370.51	2372.44	2371	
1653.00	1649.14	1648.30,1650.29,1652	H-O-H Symmetric bending vibrations
1552.70	1558.48	--------	----------
-------	1217.08	1214.20,1211.02,1217	PO4 P=O associated stretching vibrations
1136.07	**1136.07**	1136.70,1129.96,1134	PO4 bond, P=O stretching vibrations
1064.71	1062.78	1062.30,1064.34,1065	
987.55	**987.55**	987.20,989	P-O-P asymmetric stretching bond
873.75	**873.75**	874.1,873.10,872	
790.81	792.74	792.0,705.00,795	
665.44	661.58	664.00,666	(H-O-) P=O bond (strong absorption) acid phosphates
-------	576.72	577.1,576.30,577	
528.50	**528.50**	527.7,525.71,527	

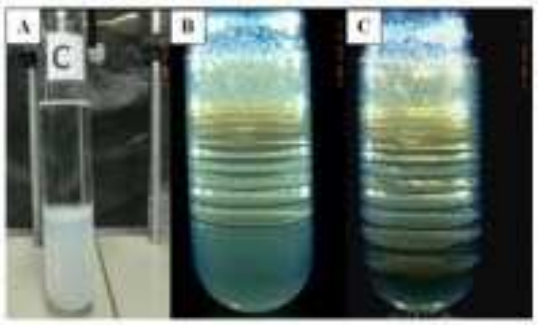

Figure 1: Liesegang rings formation during brushite crystals growth (A) No ring observed on 1st day, (B) 10 rings on 2nd day and (C) 12 rings on 3rd day.

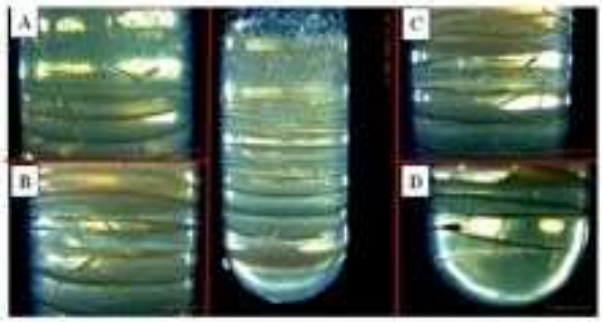

Figure 2: Brushite crystals grown in gel medium (A) upper portion, (B and C) middle portion and (D) lower portion of test tube.

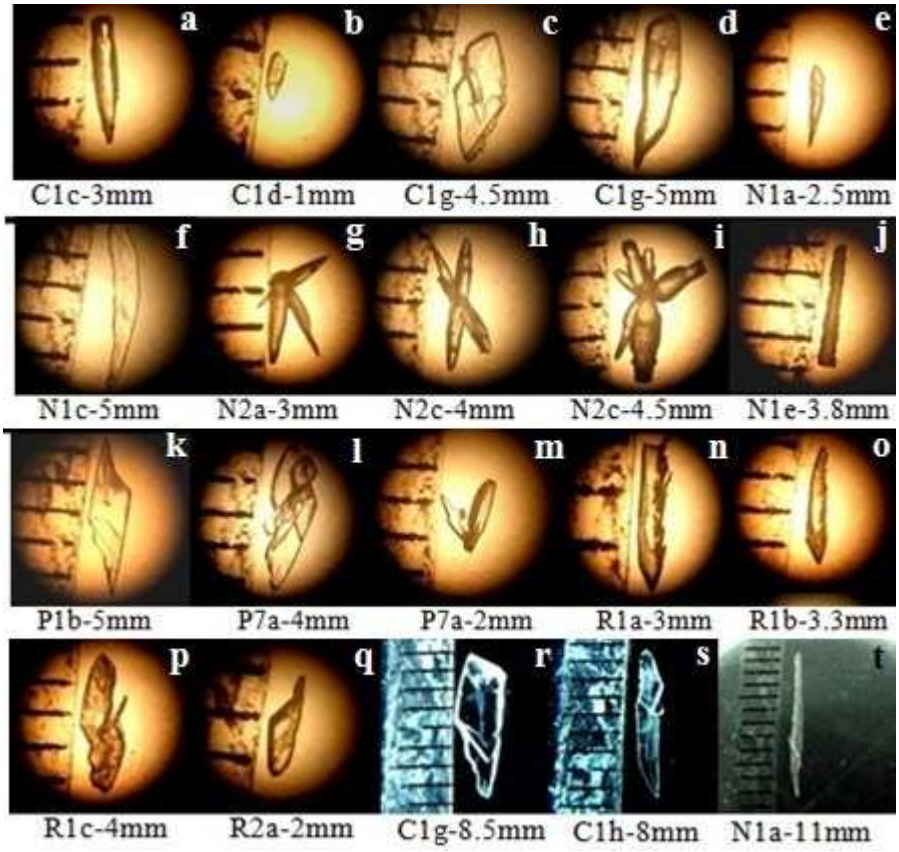

Figure 3: Measured brushite crystals of different morphologies. Microphotographs with 10x magnification (a-q) and photographs without microscope (r-t).

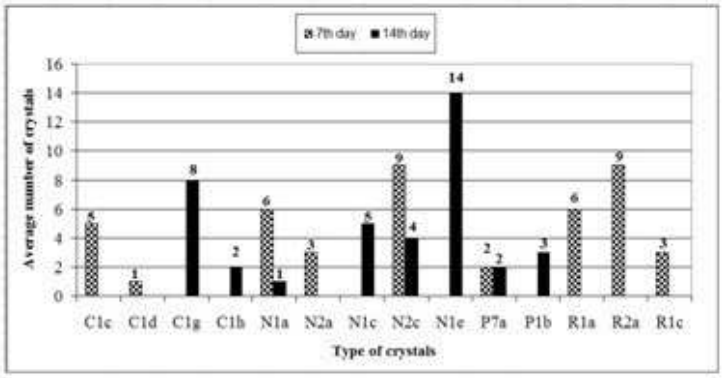

Figure 4: Different types of brushite crystals with their average number observed at 7th and 14th day

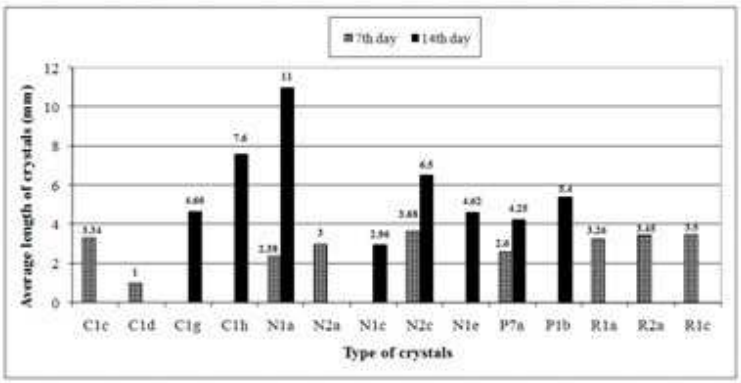

Figure 5: Different types of brushite crystals with their average length (mm) observed at 7th and 14th day

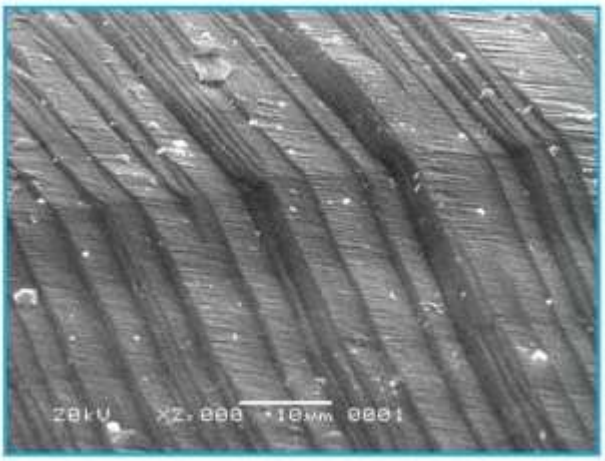

Figure 6: SEM image of completely grown brushite crystal at 10 μm.

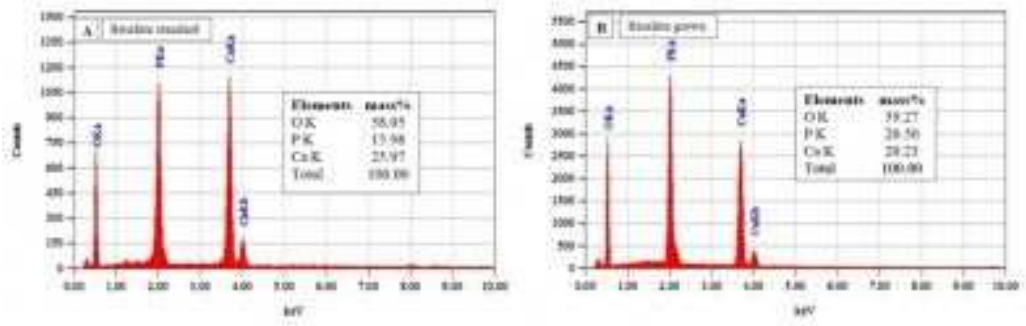

Figure 7: EDS analysis of brushite crystals. (a) standard and (b) grown.

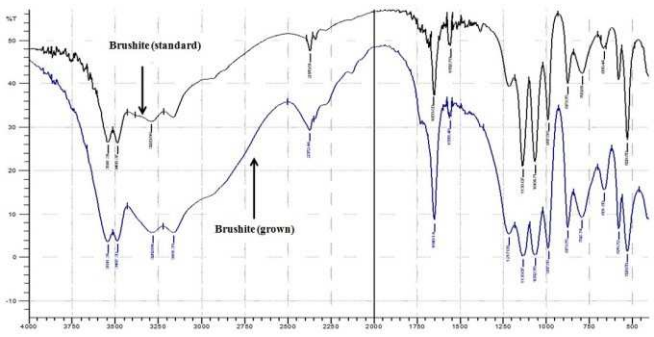

Figure 8: FT-IR spectra of completely grown brushite crystals.

RESULTS AND DISCUSSION

Brushite crystals were observed as bullet, columnar, needle and platy crystals and their aggregates (Figure 1-3). Weight of harvested crystals, their morphology and density (crystal crowd) are shown in Table-1 and Figure 4-5. The SEM images are shown in Figure-6. EDS spectrum of testing and standard samples shows the matched mass percentage of detecting elements. The average mass % of the elements is calcium 20.23, phosphorus 20.50 and oxygen 59.27. The values of standard compounds are calcium 25.97, phosphorus 15.98 and oxygen 58.05% (Figure 7). The FT-IR spectra compared with the spectra of commercially available compound and previously reported values (Table 2; Figure 8).

Morphological features of harvested crystals are described according to Magono and Lee meteorological classification[12]. Brushite crystals were observed in different shapes and sizes. Column shape crystals were dominant in number and needle shaped in length. The diffusion of ions through the gel medium results insoluble precipitates in the form of Liesegang ring. Each ring contains numerous nuclei participative in crystal formation. The number of rings increased with time and total twelve rings were observed. The SEM photographs of brushite shows smooth surface with complete sheet like morphology (Figure-6). The EDS measurements were made at different points on the crystal surface. The results indicate that the crystals are composed of primarily calcium, phosphate and oxygen. The less difference of mass percentages between grown crystals and standard compound verify the grown crystals as calcium hydrogen

phosphate dihydrate (brushite). The FT-IR resembles with that of commercially available compound and reported values (Figure 8).

The world population of about 12% suffers with urolithiasis. Everywhere throughout the world in various nations and societies, individuals utilize plants, for the aversion and cure of kidney stone as per their ethno pharmacological data. Interest in herbal drugs is growing due to their efficiency and less side effects. However, the understandings of the urolithiasis pathophysiology and pharmacology of natural medicines are of great importance for the development of safe and effective antiurolithiatic medicines[13].

The studies of crystal growth morphology are very important to understand the physico-chemical properties of crystals participating in cholelithiasis, gout and urolithiasis. In case of promotory, modulatory and inhibitory effects of additives, these studies provide an applied approach for the management and cure of these diseases[14]. This study shared detailed morphology, average size, number and weight of brushite crystals. Any type of change in these parameters will provide the sense of phosphate type kidney stone promotion, modulation and inhibition.

CONCLUSION

Brushites were observed with fourteen unique morphologies explained on the basis of Magono and Lee meteorological classification. The acquired information regarding shapes, size and average weight of crystals may be applied by incorporating extracts of natural products during crystal growth. The observed changes as compared to the control experiments will be helpful to evaluate risk factors and also devising the means for the prophylactic management of phosphate type urinary stones. The present study only shares the brushite crystal growth patterns. In future, atomic force microscopy and scanning confocal interference microscopic techniques are recommended to measure growth rates of crystals along different axes to understand the growth kinetics.

REFERENCES

1. Selvaraju R, Vasuki G. Growth of calcium hydrogen phosphate dihydrate (CHPD) crystal and characterization studied by spectral method. Int J Curr Adv Res, 2014 ; 3(10): 40-42.
2. Khan S. Animal models of kidney stone formation: an analysis. World J Urol, 1997 ; 15(4): 236-243.
3. Ratkalkar V, Kleinman J. Mechanisms of Stone Formation. Clin Rev Bone Miner Metab, 2011 ; 9(3): 187-197.
4. Grases F, Prieto R, Costa-Bauza A. *In vitro* models for studying renal stone formation: a clear alternative. ATLA: Altern Lab Anim, 1997 ; 26(4): 481-503.
5. Rajendran K, Keefe CD. Growth and characterization of calcium hydrogen phosphate dihydrate crystals from single diffusion gel technique. Cryst Res Tech, 2010 ; 45(9): 939-945.
6. Aihara K, Byer KJ, Khan, SR. Calcium phosphate–induced renal epithelial injury and stone formation: Involvement of reactive oxygen species. Kidney Int, 2003 ; 64(4): 1283-1291.
7. Krambeck AE, Handa SE, Evan AP, Lingeman JE. Brushite stone disease as a consequence of lithotripsy? Urol Res, 2010 ; 38(4): 293-299.
8. Siener R, Netzer L, Hesse A. Determinants of brushite stone formation: A case-control study. PloS one, 2013 ; 8(11): e78996.
9. Achilles W. *In vitro* crystallisation systems for the study of urinary stone formation. World J Urol, 1997 ; 15(4): 244-251.
10. Patel A, Rao AV. Crystal growth in gel media. Bull Mat Sci, 1982 ; 4(5): 527-548.
11. Joseph K, Parekh BB, Joshi M. Inhibition of growth of urinary type calcium hydrogen phosphate dihydrate crystals by tartaric acid and tamarind. Curr Sci, 2005 ; 88(8): 1232-1238.
12. Magono C, Lee, CW. Meteorological classification of natural snow crystals. Journal of the Faculty of Science, Hokkaido University. Series 7, Geophysics, 1966 ; 2(4): 321-335.
13. Ahmed S, Hasan MM, Mahmood, ZA. Antiurolithiatic plants: Formulations used in different countries and cultures. Pak J Pharm Sci, 2016 ; 29(6): 2129-2139.
14. Ahmed S, Hasan M, Mahmood ZA. Urolithiasis in gel: Successful journey of an *in vitro* model from vision to reality. J Pharmacogn Phytochem, 2017 ; 6(1): 102-108.
15. Sekar C, Suguna K. Effect of H3PO4 reactant and NaF additive on the crystallization and properties of brushite. Adv Mat Lett, 2011; **2**(3): 227-232.
16. Diana K, George K. Urinary stone formation: Efficacy of seed extract of *Ensete superbum* (Roxb.) Cheesman on growth inhibition of calcium hydrogen phosphate dihydrate crystals. J Cryst Growth, 2013; 363: 164-170.

How to cite this article:
Salman Ahmed *et al*. Phosphate type kidney stone (Brushite) formation in gel: A morphological study on growth patterns. J Pharm Sci Innov. 2017;6(3):64-68.

Source of support: Nil, Conflict of interest: None Declared